Korean J. Chem. Eng., 36(9), 1499-1508 (2019)
DOI: 10.1007/s11814-019-0335-6

pISSN: 0256-1115
eISSN: 1975-7220

Transformation and coagulation behaviors of iron (III) species of solid polymeric ferric sulfate with high basicity

Dan Li, Yong Kang†, Jie Li, and Xin Wang

School of Chemical Engineering and Technology, Tianjin University, Tianjin 300350, China
(*Received 2 March 2019 • accepted 3 July 2019*)

Abstract−Solid polymeric ferric sulfate (SPFS) with excellent solubility and high basicity up to 20.16% was prepared employing hydrogen peroxide as oxidizer via acid deficient method. The transformation and size distribution of iron (III) species in the stock solution of SPFS ($SPFS_{sto}$) were investigated, and coagulation behavior of iron (III) species in surface water was explored as well. It was found that the as-prepared SPFS with a high basicity was of high total iron content about 24.55% with an amorphous structure. The iron (III) species in $SPFS_{sto}$ suffered complicated behavior during aging and dilution, in which both further polymerization and depolymerization were included, the average diameters of iron (III) species in $SPFS_{sto}$ varied from 1 nm to 4 nm and decreased with the increase of R value at the total iron concentration of 1.0 M, and became more dispersed at the total iron concentration of 1.0 mM. The distribution of iron (III) species in surface water used in experiment depended on the initial pH value of the coagulation system and transformed during coagulation. In general, the low polymer of iron (III) species Fe_a dominated in acidic system, while the medium ones Fe_b and the high ones Fe_c dominated in neutral and basic systems, respectively. Charge neutralization and complexation by Fe_b species were found to be the most efficient mechanisms in removal of high molecular weight hydrophobic organics, and absorption and sweeping capabilities of Fe_c species dominated in removing low molecular weight hydrophilic organics.

Keywords: Solid Polyferric Sulfate, High Basicity, Acid Deficiency Method, Iron (III) Species, Surface Water

INTRODUCTION

Polyferric sulfate (PFS) is a type of pre-polymerized inorganic coagulant developed in the 1980s with the general formula $[Fe_2(OH)_n(SO_4)_{(3-n/2)}]_m$ (0<n<2, m>10) [1]. It has been widely used in water treatment because PFS is non-toxic and environmentally friendly compared to alum-salt coagulants such as poly-aluminium chloride (PAC). For the convenience of transportation and storage, PFS is mostly prepared as solid powders (SPFS) instead of liquid products (LPFS). However, most of the commercial SPFS products have excess insoluble content, including iron hydroxide or sodium jarosite [2]; these components cannot function during the coagulation operation but can easily adhere to the inner wall of the containers causing the equipment corrosion. Besides, the commercial products of SPFS have lower active polymerized components, leading to a high addition dosage and a large amount of residues during coagulation process. Therefore, developing SPFS with higher activity is inevitable.

It is generally agreed that prolonged overheating during preparation adversely affects the polymerization of SPFS, as well as its structure [3,4]. So liquid PFS (LPFS) with a high concentration is preferred for the preparation of SPFS to avoid the adverse effects of high temperature. Zouboulis et al. [5] managed to prepare LPFS with high polymerization degree by adding 0.5 M $NaHCO_3$ to conduct telomerization, and its total iron content was only 47.5 g/L, lacking for commercial values. Xu et al. [6] believed that higher basicity was necessary for a better coagulation performance and managed to prepare LPFS with high basicity by introducing bipolar membrane electrodialysis (BMED), but the top basicity was only 14.77%. Recently, Jia et al. [2] pointed out that sodium ions would lead to the formation of sodium jarosite and significantly reduce the stability of PFS. Therefore, to avoid the introduction of sodium ions, the acid deficiency method using hydrogen peroxide as oxidant is a reasonable choice for the preparation of high performance PFS. The process can be summarized as the following two types of reactions.

Oxidation-hydrolysis:

$$FeSO_4+\frac{1}{2}H_2O_2+\left(\frac{2-n}{4}\right)H_2SO_4 \rightarrow \frac{1}{2}\left[Fe_2(OH)_n(SO_4)_{3-\frac{n}{2}}\right]+\left(\frac{2-n}{2}\right)H_2O \quad (1)$$

Polymerization:

$$m\left[Fe_2(OH)_n(SO_4)_{\frac{3-n}{2}}\right]\rightarrow\left[Fe_2(OH)_n(SO_4)_{\frac{3-n}{2}}\right]_m \quad (2)$$

In general, a large n value (0<n<2) can embody a high polymerization degree of PFS [6-8]; therefore, the effective regulation on the polymerization degree of PFS can be achieved by strictly controlling the added dosage of H_2SO_4. For the convenience of discussion, the parameter R (0<R<0.5) was defined to substitute (2−n)/4, which is the stoichiometric ratio of H_2SO_4 to $FeSO_4$ in Eq. (1).

There are a variety of aggregated species of iron (III) in the aque-

†To whom correspondence should be addressed.
E-mail: ykang@tju.edu.cn

ous solution of PFS. According to the reaction rates between different iron (III) components and Ferron reagents, the Fe (III) species in the solution can be divided into monomers (Fe_a), medium polymers (Fe_b) and high polymers (Fe_c), in which Fe_a reacts with the Ferron reagents within 1 minute, including Fe^{3+}, $Fe(OH)^{2+}$ and $Fe(OH)_2^+$ etc. Fe_b is the component that reacts with Ferron subsequently until the absorbance at 600 nm is substantially constant, including $Fe_2(OH)_2^{4+}$, $Fe_3(OH)_4^{5+}$ and $Fe_8(OH)_{20}^{4+}$ etc. Fe_c cannot participate in the reaction with Ferron [9,10]. The coagulation performance of iron-based coagulants is closely related to the content of different iron (III) species [11]. Lei et al. [12] claimed that the iron (III) species with higher positive charge density in polyferric chloride (PFC) were the most efficient components for removing humic acid. Dong et al. [13] pointed that the more Fe_a and Fe_b in PFC, the more easily it is to form large and fluffy flocs, and thus resulting in less membrane fouling. However, an uncertainty exists in the transformation of iron (III) species in the stock solution of SPFS ($SPFS_{sto}$). Furthermore, stirring conditions, pH and the existence of impurities in raw water during coagulation will also have a direct effect on the distribution of iron (III) species and the coagulation performance [14-16]. Nevertheless, the transformation behavior of iron (III) species during coagulation operation by dosing $SPFS_{sto}$ have rarely been reported till now.

In this paper, high basicity SPFS with excellent solubility was prepared via the acid deficiency method, and the characteristics of SPFS were studied. Moreover, the transformation of different iron (III) species in $SPFS_{sto}$ and raw water was investigated as well, and coagulation behavior of different iron (III) species was explored eventually.

MATERIALS AND METHODS

1. Chemical Reagents and Water Samples

All the reagents used in this study such as $FeSO_4 \cdot 7H_2O$, H_2O_2, and H_2SO_4 of analytical grade were provided by Rianlon Corporation, Tianjin, China. Three commercial SPFS samples used in this study were purchased from three chemicals companies, respectively, the suppliers and preparation methods are listed in Table 1. The real surface water was taken from the Youth Lake of Tianjin University in May, 2018. The quality of the water sample in the experiment is shown in Table 2.

2. Preparation of PFS

A certain amount of $FeSO_4 \cdot 7H_2O$ was added in an equal amount into seven 250 mL three-necked flasks with stirring function, corresponding amount of H_2SO_4 was added into the flask according to a certain R value (0.2, 0.25, 0.3, 0.35, 0.4, 0.45 and 0.5), followed by 5 mL of deionized water. Then the above suspension was stirred at 125 rpm under 60 °C for 30 min until it became a slurry. H_2O_2 was added dropwise into the slurry under continuous stirring at about 200-250 rpm. To prevent H_2O_2 from being thermally decomposed, the reactor temperature was maintained at about 30 °C with cooling water during the oxidation reaction. The content of ferrous iron was titrated with $KMnO_4$ standard solution of $c(1/5KMnO_4)$= 0.01 M every 20 min during the reaction until the concentration of Fe (II) was less than 0.1 wt%, then a raw liquid PFS solution was obtained. To prepare the SPFS, the LPFS was heated and concentrated under normal pressure, then the concentrated samples were dried at 80-90 °C in a constant temperature oven for about 4 h. The SPFS powder was obtained by grinding the dried sample in a mortar for 30 min.

3. Analysis and Characterization of PFS

3-1. Determination of the Active Components in PFS

To evaluate the activity of the PFS samples obtained, the total iron content, the ferrous iron content, the insoluble substance content and the basicity were measured and calculated as described in the previous literature [6].

3-2. Analysis of XRD, SEM and Size Distribution

The XRD patterns were measured by an X-ray diffractometer (X'Pert Pro, PANalytical Co. Ltd., Netherlands) with a scanning range from 10 to 80° and a scanning speed of 4°/min. The SEM images were photographed with scanning tunneling electron microscopy (S-4800, Hitachi Co. Ltd., Japan). The size distribution of iron (III) species in the PFS solution was measured by a nano-laser particle size analyzer (Zetasizer Nano ZS, Malvern Instruments Co. Ltd., UK).

3-3. The Distribution of Iron (III) Species of PFS_{sto}

A certain amount of the PFS samples (LPFS or SPFS) were dissolved in deionized water to obtain different concentrations of PFS_{sto}. The exact concentration of total iron ([TFe]) was measured by the 1,10-phenanthroline spectrophotometry [5]. After aging for different periods (0, 4, 8, 12, 16 and 24 h), the iron (III) species in the PFS_{sto} was determined by Fe-Ferron method as described in the previous literature [5,13,18]. A UV-Vis spectrophotometer (L6S, INESA Analytical Instrument Co. Ltd., China) was used to record the variation of the maximum absorbance at 600 nm, in which the absorbance observed within 1 min was corresponding to Fe_a content ([Fe_a]), the absorbance from 1 min to the constant absorbance

Table 1. The suppliers and preparation methods of three commercial SPFS samples used in this work

Sample type	Supplier	Preparation method
Commercial SPFS 1	Qingyuan Environmental Protection Products Co., Ltd., Tianjin, China	Nitric acid oxidation-alkali telomerization
Commercial SPFS 2	Dongmao Environmental Protection Material Co. Ltd., Xinxiang, China	Sodium chlorate oxidation
Commercial SPFS 3	Yuanli Chemical Co. Ltd., Tianjin, China	Sodium nitrite catalytic-oxidation

Table 2. Quality of the test water sample in the jar tests

Types of water samples	pH	Turbidity (NTU)	Zeta potential (mV)	UV_{254} (/cm)	DOC (mg/L)	SUVA ($100 \times UV_{254}$/DOC)
Surface water	8.27	11.48	-37.37	0.1048	6.851	1.530

Table 3. Typical properties of the LPFS prepared by acid deficiency method

R value	[TFe] (wt%)	[Fe^{2+}] (wt%)	Basicity (%)	pH (1 wt%)	Density ($\times 10^3$ kg/m^3)	Viscosity (cp, 20 °C)
0.20	14.63	0.01	20.14	2.43	1.75	98
0.25	14.24	0.02	17.66	2.34	1.76	110
0.30	13.80	0.01	13.94	2.33	1.76	116
0.35	13.74	0.01	10.10	2.24	1.77	118
0.40	13.62	0.03	7.11	2.15	1.77	124
0.45	13.38	0.02	4.44	2.12	1.77	125
0.50	13.19	0.01	0.34	2.01	1.78	127

Table 4. Comparison of the properties of the SPFS samples prepared in this work with the commercial products

Sample type	Sample No.	[TFe] (wt%)	Basicity (%)	pH (1 wt%, sol)	Insoluble substance content (wt%)
R=0.20	A	24.55	20.16	2.41	0
R=0.25	B	23.92	17.70	2.36	0
R=0.30	C	23.81	13.50	2.32	0
R=0.35	D	22.92	10.24	2.25	0
R=0.40	E	22.26	7.23	2.21	0
R=0.45	F	21.91	4.02	2.13	0
R=0.50	G	21.17	0.54	2.05	0
Commercial SPFS 1	H	20.73	13.88	2.26	2.08
Commercial SPFS 2	I	20.36	17.28	2.31	0.35
Commercial SPFS 3	J	20.29	14.52	2.29	0.43

(about 6 to 12 h) was corresponding to Fe_b content ([Fe_b]), and the Fe_c content ([Fe_c]) was calculated by the formula of [Fe_c]=[TFe]−[Fe_a]−[Fe_b].

3-4. Coagulation Performance

Coagulation performance of PFS was evaluated by jar tests for the treatment with real surface water. The jar tests were carried out at room temperature using a six-peddle agitator (MY3000-6M, Meiyu Instrument Co. Ltd., China). The PFS_{sto} solution with the concentration of [TFe]=1.0 M was prepared using LPFS or SPFS and deionized water 12 h prior to the jar tests. 250 mL water sample pre-adjusted to a specified pH value was transferred into a 500 mL beaker, then a certain amount of PFS_{sto} was added into the beaker by a pipette under rapid stirring conditions. After the steps, rapid stirring at 200 rpm (G=187.8 s^{-1}) was applied for 30 s, followed by slow stirring at 30 rpm (G=10.9 s^{-1}) for 15 min. Finally, the coagulated water sample settled for 20 min. Once the rapid stirring period was completed, a certain amount of water sample in the beaker was taken to determine the zeta potential using a micro-electrophoresis apparatus (JS94H, Shanghai Zhongchen Digital Equipment Co. Ltd., China).

After the settlement was completed, the supernatant was taken immediately for measurements of its residual turbidity, UV_{254} and DOC. The residual turbidity was measured directly using a turbidimeter (WGZ-100, Shanghai Optical Instrument Co. Ltd., China). The UV_{254} and DOC values of the supernatant filtrated with a 0.45 μm membrane were tested by the UV-Vis spectrophotometer at 254 nm and a TOC analyzer (TOC-L, Shimadzu Co. Ltd., Japan), respectively. Additionally, the iron (III) species in the coagulated water samples at different coagulation periods in a jar experiment were tested by the Fe-Ferron method.

RESULTS AND DISCUSSION

1. Characteristics of PFS Prepared by the Acid Deficiency Method

The as-prepared samples of LPFS and SPFS were obtained by the acid deficiency method. The typical properties of the fresh LPFS samples are listed in Table 3. The total Fe content, basicity and pH values of LPFS (1%, sol) decrease with the increasing of R values, while the density and the viscosity increase slightly. It can be seen that the total Fe content of LPFS samples without concentration ranges from 13.19 to 14.63%, and its top basicity reaches 20.14%, which is obviously higher than the highest value reported in the previous literature [6]. Table 4 summarizes the differences between the SPFS obtained in this work (Sample A-G) and three commercial products (Sample H-J). It is observed that the top basicity of Samples A reached 20.16% when R was 0.2, while the basicity of Sample H-J was only about 13.88-17.28%. Note that none of the insolubles are detected in Samples A-G, while a maximal content of insolubles exists in Sample H, which is prepared by nitric acid oxidation-alkali telomerization method. The crystalline phases of SPFS dried from LPFS with a high concentration are shown in Fig. 1. All the samples with different R values have largely amorphous structures with small traces of crystallinity as shown in Fig. 1(a), suggesting that the R value has no effect on the structure of SPFS prepared by acid deficiency method. The XRD patterns in Fig. 1(a) show two common broad diffraction peaks around the 2θ values of 13.74° (d=0.644 nm) and 25.71° (d=0.346 nm), corresponding to the hydrated ferric sulfate and the basic hydrated ferric sulfate, respectively. It suggests that the SPFS sample was s mixture of a series of hydrated ferric sulfate and basic hydrated ferric sulfate.

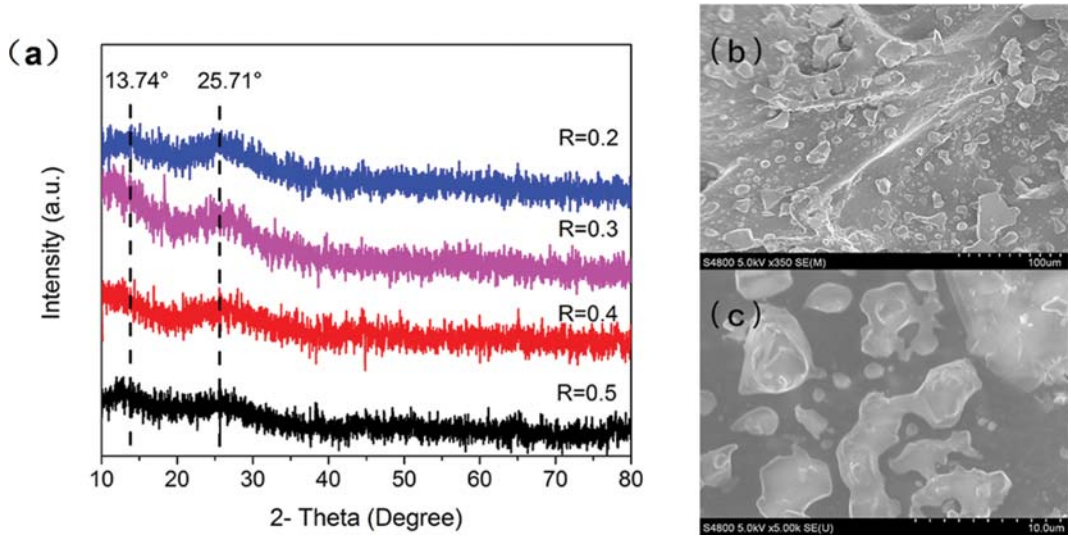

Fig. 1. Characterization of SPFS prepared by acid deficiency method with different R values: the XRD patterns of SPFS (a) and the SEM images of Sample A (b) and Sample E (c).

The amorphous structures of Samples A and E are also supported by the SEM images in Fig. 1(b) and Fig. 1(c), the random arranged structures contribute a large specific surface area of SPFS; therefore, it is more reactive in coagulation process.

2. Distribution of Iron (III) Species in $SPFS_{sto}$

2-1. Differences in the Distribution of Iron (III) Species between $SPFS_{sto}$ and $LPFS_{sto}$

The solutions of $SPFS_{sto}$ and $LPFS_{sto}$ with 1 M of [TFe] were prepared, respectively, by deionized water and aged for 12 h at room temperature before the measurement of iron (III) species. It can be seen in Fig. 2 that the distribution of iron (III) species in the solution of $SPFS_{sto}$ or $LPFS_{sto}$ was determined by R value. The smaller the R value, the lower the content of Fe_a, and the higher those of Fe_b and Fe_c. Notably, the total content of Fe_b and Fe_c in $SPFS_{sto}$ was higher compared with in $LPFS_{sto}$ at the same R value, especially the Fe_b content, indicating that the hydrolysis and polymerization of iron (III) ions were continued in the drying process. Similar results were obtained by Zheng et al. [19]. It is shown in Fig. 2 that the maximum content of Fe_b in the solution of $SPFS_{sto}$ is 35.18% at R=0.20, the content of Fe_c is also appreciable. The Fe_b species is the most effective component with a stronger charge neutralization capacity [13]. Nevertheless, the Fe_c species which are amorphous with huge specific surface area also play an important role for the absorption ability of PFS during the coagulation [20]. Therefore, the SPFS sample with R=0.2 was selected for the next experiments.

2-2. Effect of Aging Time on the Transformation of Iron (III) Species in $SPFS_{sto}$

The transformation of iron (III) species in $SPFS_{sto}$ (R=0.2, [TFe]= 1.0 M) as a function of aging time was investigated, and the pH value of the solution was monitored simultaneously. The results are presented in Fig. 3. At the first four hours of the aging period, the Fe_a content decreases slightly while the Fe_b content increases from 18.12 to 32.09%, and the Fe_c content decreases from 16.33 to 6.54%. About eight hours later, there is a greater decrease in the

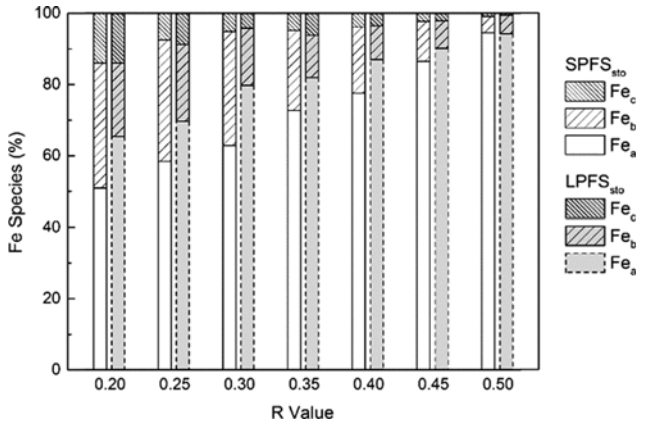

Fig. 2. Distribution of iron (III) species in $SPFS_{sto}$ and $LPFS_{sto}$.

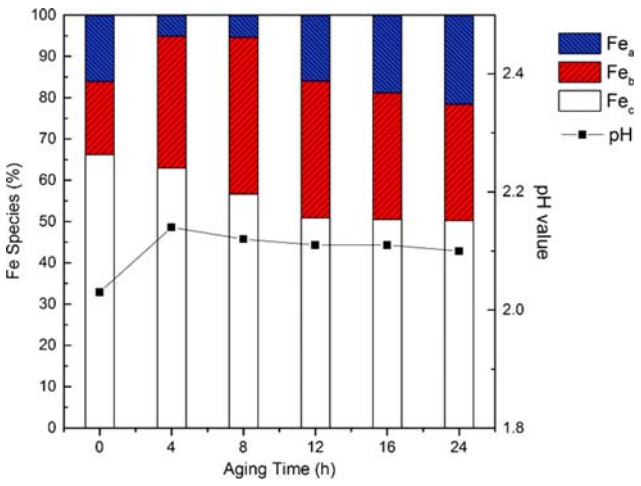

Fig. 3. Distribution of iron (III) species in $SPFS_{sto}$ (R=0.2, [TFe]= 1.0 M) during the aging period.

Fe_a content, and the Fe_b content increases substantially to its maximum (37.68%). In the following sixteen hours, little change takes place in the Fe_a content, while the Fe_b content decreases continually and the Fe_c content is accumulated from 6.22 to 15.38%. The pH value of the SPFS solution increases significantly at the first four hours, and then decreases steadily as the function of aging time. All the results above suggest that a complicated process of the transformation of iron (III) species occurs during the aging period of $SPFS_{sto}$. When the SPFS is dissolved initially, a decrease in the polymerization degree of the coordination compounds takes place as the iron (III) species diffuse into water, which can be explained by the theory of coordination chemistry that the lower the concentration of the metal complex, the lower the degree of polymerization of the coordination compound is [21-23]. Fig. 4 illustrates the hydrolysis-polymerization process of iron (III) species, which was proposed by Dousma et al. [24,25]. Considering the sharp decline of the Fe_c content and the remarkable increase of the Fe_b content at the first four hours, it can be inferred that breakage takes place in Fe-O-Fe bonds as shown in the group structure E of Fig. 4 during the diffusion of iron (III) species and then converts into the structure D with Fe-OH-Fe bonds by complexing with H^+ in water, resulting in an increasing of the pH value of the solution simultaneously. This inference could be confirmed by Hellman et al. [26], who found the stability of the oxo-bridged structures was lower than that of the hydroxo-bridged structures in the solution.

2-3. Effect of Dilution on the Transformation of Iron (III) Species in $SPFS_{sto}$

Based on the discussion above, it's known that depolymerization of iron (III) species would happen when the concentration of iron (III) complexes decreased, so the polymerization degree of iron (III) species is bound to decline when $SPFS_{sto}$ is diluted in water. Conversely, the pH value of deionized water is generally much higher than that of $SPFS_{sto}$, so dilution of $SPFS_{sto}$ with deionized water is equivalent to the addition of alkali in a sense, and the polymerization of the iron ions is promoted with the spontaneous hydrolysis as a result. To quantify the hydrolysis extent of iron (III) ions in the stock solution of SPFS prepared by acid deficiency method, the average number of OH^- bounded with one iron (III) ion was calculated with the following equation defined in this work.

$$B^* = B_P + B_H \tag{3}$$

where B^* represents the exact average number of OH^- bounded with one iron (III) ion in the $SPFS_{sto}$, calculated by $B^* = [OH]_{bound}/[TFe]$; B_p is the theoretical average number of OH^- bounded with one iron (III) ion in solid PFS, calculated by $B_p = 1-2R = n/2$ from the SPFS formula of $[Fe_2(OH)_n(SO_4)_{3-n/2}]_m$; B_H refers to the average number of extra OH^- bounded with one iron ion due to the spontaneous hydrolysis of iron species in the solution [27], calculated with $B_H = 10^{-pH}/[TFe]$ for $SPFS_{sto}$.

Therefore, the value of B^* can also be calculated by Eq. (4) transformed from Eq. (3).

$$B^* = 1 - 2R + \frac{10^{-pH}}{[TFe]} \tag{4}$$

To estimate the spontaneous hydrolysis extent of iron (II) species, the values of pH and B_H for $SPFS_{sto}$ ([TFe]=1.0-1.0×10^5 mg/L) were determined after 12 h aging; the results are shown in Fig. 5. It can been seen that the value of B_H increases with the increas-

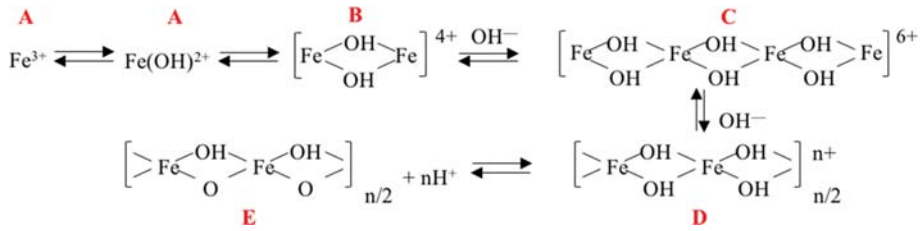

Fig. 4. Dousma model based on the conversion of Fe(III) species.

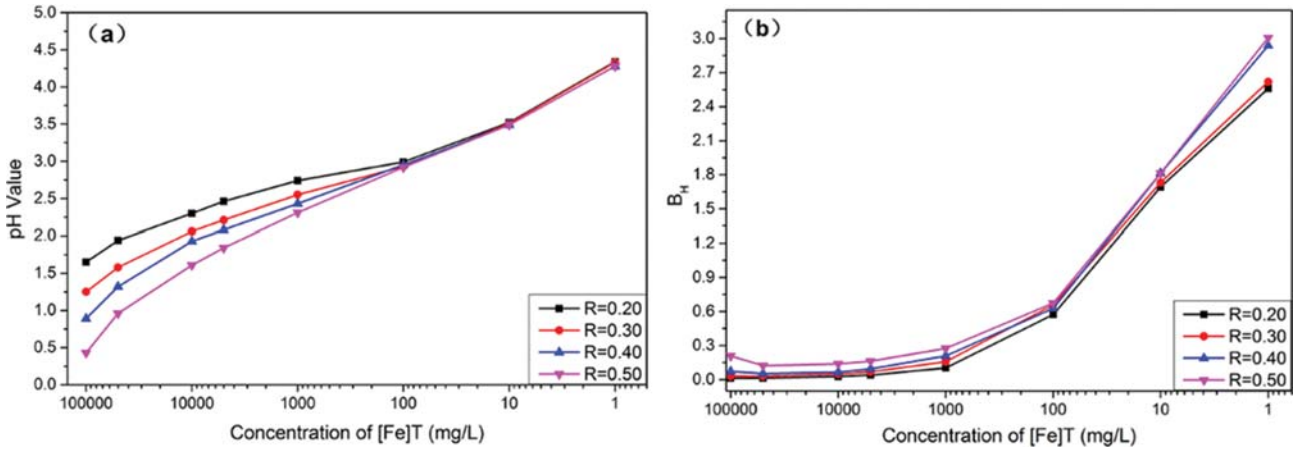

Fig. 5. The spontaneous hydrolysis ability of $SPFS_{sto}$ with different R values: the values of pH (a) and B_H (b).

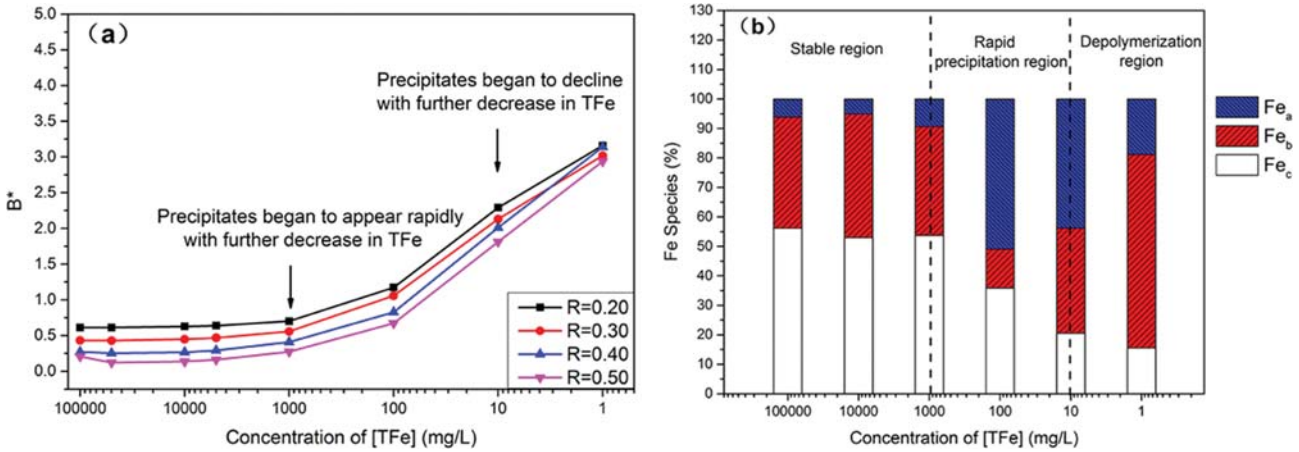

Fig. 6. Effect of [TFe] on the values of B^* of $SPFS_{sto}$ with different R values (a) and the distribution of Fe(III) species of the $SPFS_{sto}$ at R=0.2 (b).

ing of R value, which means that the greater the content of Fe_a the stronger spontaneous hydrolysis capability the $SPFS_{sto}$ had. The pH value of $SPFS_{sto}$ increases continually as the decreasing of [TFe], while the value of B_H first remains stable at the range of [TFe] between 1.0×10^3 to 1.0×10^5 mg/L and then increases tremendously with the further decrease of [TFe]. That is because the pH value of $SPFS_{sto}$ with a high [TFe] is so low that it inhibits the hydrolysis of iron (III) ions.

Effect of [TFe] on the stability of $SPFS_{sto}$ is evaluated by the parameter B^* and the distribution of iron (III) species, as shown in Fig. 6. Three regions are divided depending on the precipitation phenomena of $SPFS_{sto}$. Both B^* and the content of iron (III) species are relatively stable at the region of [TFe] between 1.0×10^3 to 1.0×10^5 mg/L, as known that high concentration of PFS solution is corresponding with a higher viscosity [6], so the relatively high content of Fe_a (about 55.27%) in the solution as shown in Fig. 6(b) suggests that high viscosity of the solution has an adverse impact on the diffusion of iron (III) species that they cannot complex with adequate monomers to get a higher hydrolysis degree. The value of B^* and the content of Fe_c all increase significantly when the content of TFe is between 10 to 1.0×10^3 mg/L, at which precipitates appear in $SPFS_{sto}$. The XRD patterns of the precipitates are shown in Fig. 7(a), in which the strong diffraction peak at $2\theta=35.77^o$ is corresponding to the ferrihydrite (PDF No. 29-0712), which belongs to hydrous iron oxides with scarcely any charges, and its spherical structure is shown in Fig. 7(b). However, when [TFe]≤10 mg/L, in spite of a high value of B^*, the precipitates decrease, even disappear at [TFe]=1 mg/L, and the content of Fe_b increases while the content of Fe_c decreases remarkably, which indicates that the depolymerization of iron (III) species becomes dominant. Under these circumstances, the macromolecules of iron (III) species are converted into smaller ones due to the conversion of the oxo-bridged structures into the hydroxo-bridged structures.

2-4. The Size Distribution of Iron (III) Species of $SPFS_{sto}$

The size distribution of iron (III) species in the stock solution of SPFS is listed in Table 5. It can be seen that the average diameters of iron (III) species of $SPFS_{sto}$ vary from 1.0 nm to 4.0 nm and decrease with the increase of R value at [TFe]=1.0 M, which is consistent with the value variation of B^* at different R levels. When the $SPFS_{sto}$ is diluted to 1.0 mM, the average sizes of iron (III) species in th stock solution increase significantly compared with those at [TFe]=1.0 M, suggesting that a higher polymerization degree is achieved by dilution of $SPFS_{sto}$. Besides, the average sizes of the iron (III) species of $SPFS_{sto}$ increase and become more dispersed at

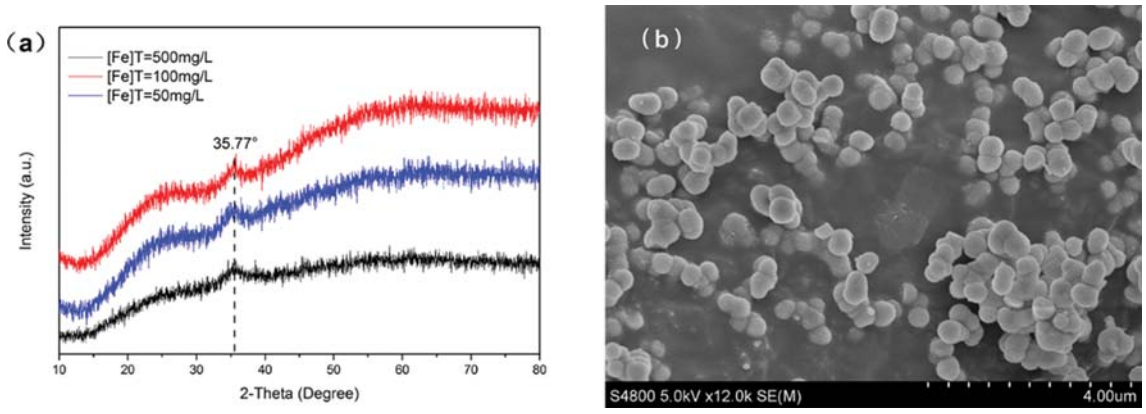

Fig. 7. The XRD patterns of the precipitates in the $SPFS_{sto}$ with different [TFe] (a) and the SEM images of the precipitates in the $SPFS_{sto}$ at [TFe]=100 mg/L(b).

Table 5. The size distribution of the iron (III) species in $SPFS_{sto}$

R	[TFe]=1.0 M			[TFe]=1.0 mM		
	Sizes (nm)	Content (%)	Average size (nm)	Sizes (nm)	Content (%)	Average size (nm)
0.2	0.6-4.0 91.0-615.0	78.7 21.3	3.6	0.7-2.7 91.0-266.0	24.9 75.1	134.2
0.3	0.6-4.0 190.0-639.0	85.1 14.9	1.9	0.6-3.0 50.0-531.0	41.3 58.7	211.4
0.4	0.5-1.7 173.0-1115.0	88.1 11.9	1.4	0.7-3.7 255.0-1002.0	42.6 57.4	480.2
0.5	0.7-4.0 202.0-1106.0	97.6 2.4	1.0	0.7-2.6 232.0-1106.0 1990.0-2669.0	36.6 60.2 3.2	616.9

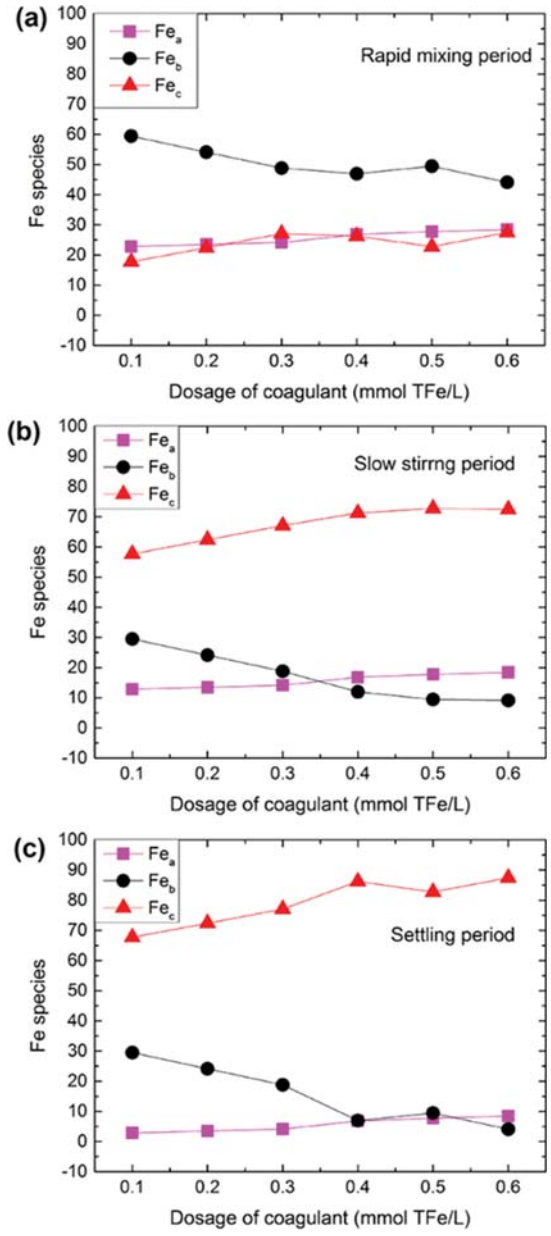

Fig. 8. Effect of dosage of $SPFS_{sto}$ on the distribution of iron (III) species in the surface water at the initial pH value of 8.27.

[TFe]=1.0 mM.

3. Transformation and Coagulation Performance of Different Iron (III) Species of $SPFS_{sto}$ for Surface Water Treatment

3-1. Effect of the $SPFS_{sto}$ Dosage

Fig. 8 shows the distribution of iron (III) species for three coagulation periods with the dosage of $SPFS_{sto}$ ([TFe]=1.0 M, R=0.2), ranging from 0.1 to 0.6 mM when the initial pH value of surface water is 8.27. The results indicate that the dosage of $SPFS_{sto}$ significantly affects the distributions of iron (III) species, especially the content of Fe_b and Fe_c. As indicated, the Fe_b content is much higher throughout the whole coagulation process when the flocculant dosage is lower than 0.4 mM. The less hydrolyzed iron (III) species is left in the supernatant water when the content of total iron is pretty low, while the generation of the highly polymerized iron (III) species tends to dominate at the dosage range of 0.4-0.6 mM. Fig. 9 shows the quality of supernatant water treated by $SPFS_{sto}$ ([TFe]=1.0 M, R=0.2) with different dosages. It is generally believed that complexation and charge neutralization dominate in the region where the zeta potential remains negative, i.e., Region I; adsorption and sweeping are dominant when the zeta potential is relatively stable, i.e., Region II; and restabilization happens when the zeta potential turns to rise significantly, i.e., Region III. It is shown in Fig. 9(a) that the content of total residual iron at lower doses of 0.1-0.3 mM is extremely higher than that of the moderate dosages; it suggests that the less polymerized species are hard to settle and thus remain in the supernatant in view of the distribution of iron (III) species in Fig. 8. The residual UV_{254}, DOC and the specific ultraviolet absorbance (SUVA) of the treated water are shown in Fig. 9(b). It shows that the high molecular weight hydrophobic organics (HHo) are more easily removed at low dosages of $SPFS_{sto}$, and then the low molecular weight hydrophilic organics (LHi) are removed at moderate dosages. Thus, the HHo is more easily removed, obeying the coagulation mechanism of complexation and charge neutralization, while the LHi is significantly removed abiding the mechanism of adsorption and sweeping.

3-2. Effect of pH Value

The transformations of iron (III) species under different initial pH conditions at the dosage of [TFe]=0.4 mM were investigated and shown in Fig. 10. It is confirmed in Fig. 10(a) that a degraded process occurs in iron (III) species once PFS is dosed into surface water with a low pH value; on the contrary, a polymerization pro-

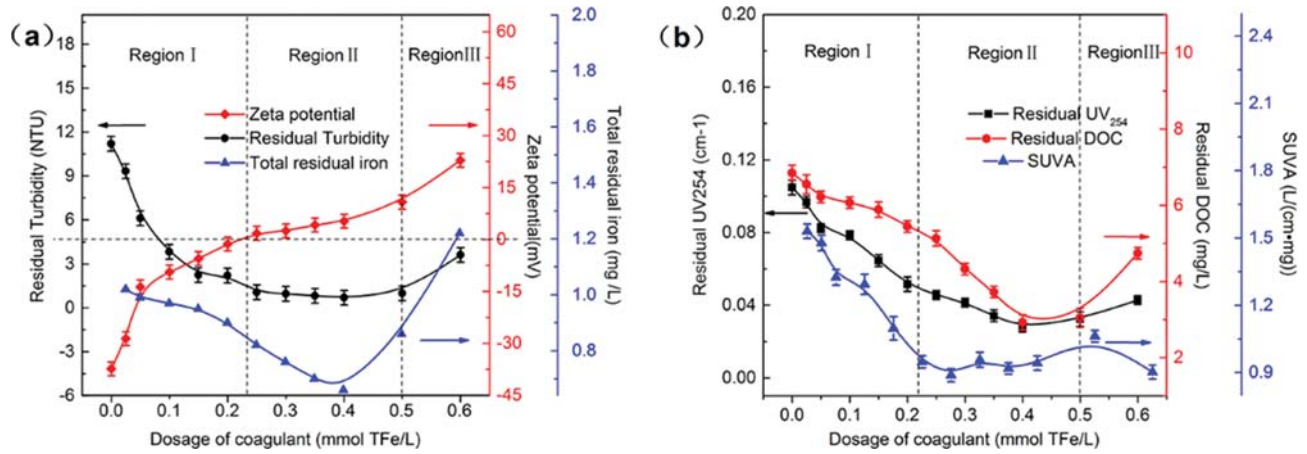

Fig. 9. Effect of dosage of $SPFS_{sto}$ on the coagulation performances for the surface water at the initial pH value of 8.27.

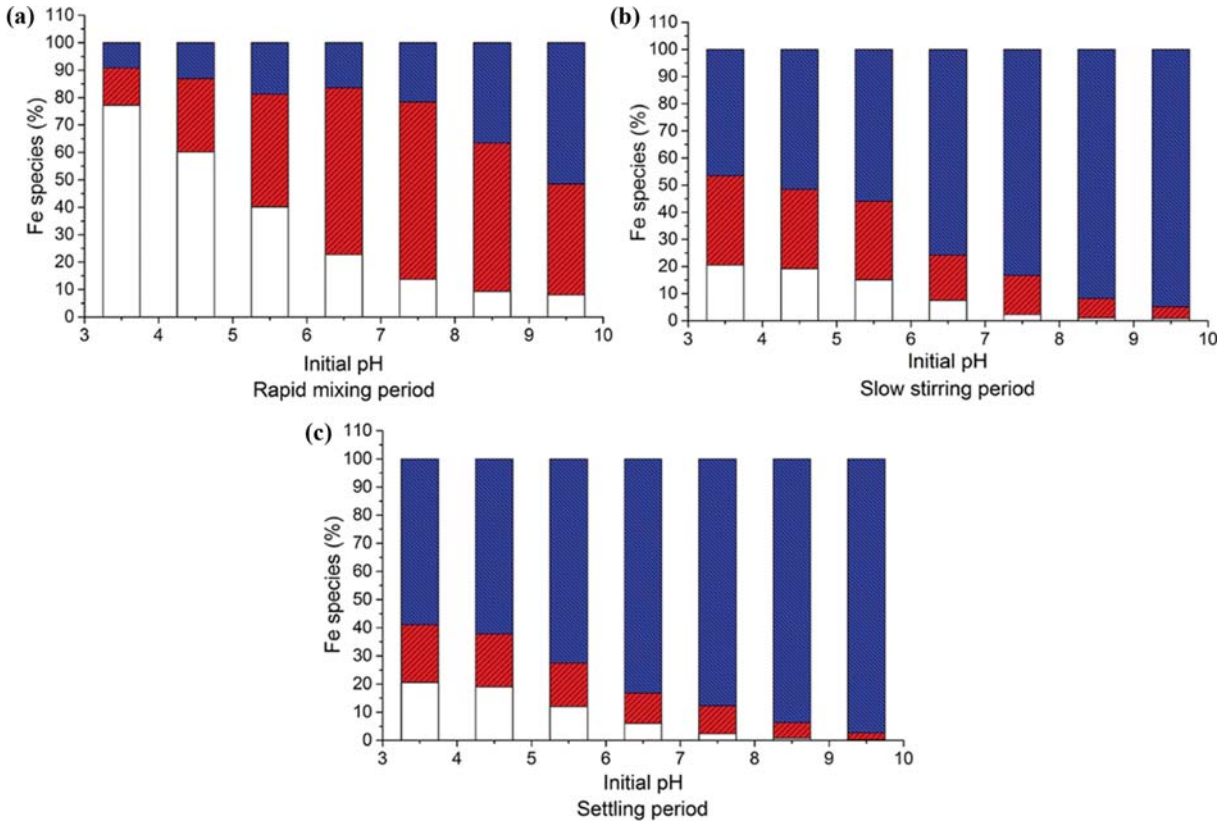

Fig. 10. Transformation of iron (III) species in the supernatant water at the dosage of [TFe]=0.4 mM.

cess of iron (III) species occurs for PFS addition into a high pH system. So at the initial coagulation period, Fe_a dominates in the acidic system, while Fe_b and Fe_c dominate in the neutral and basic system, respectively. However, at the end of slow stirring period, Fe_a suffers a great decrease about 27.12-58.33% at the pH range of 3.5-5.5, While Fe_b decreases by 55.41-67.16% at the slight acidic and neutral pH region of 6.5-7.5, and Fe_c is accumulated constantly in the whole pH range. Little change is observed in the distribution of iron (III) species at the end of flocs settling period, suggesting most of the coagulation behavior between iron species and impurities in the surface water is conducted in the slow stirring period.

As shown in Fig. 11(a), the zeta potential of flocs declines dramatically with the increase of initial pH value, suggesting that the charge neutralization ability of iron (III) species is weakened as the initial pH increases. The residual total iron content is rather high at an acidic pH region where the Fe_a species are dominant in the content, because the massive content of Fe_a at acidic pH region facilitates the formation of positively charged small impurity flocs by its spontaneous hydrolyzation, and most of the flocs are restabi-

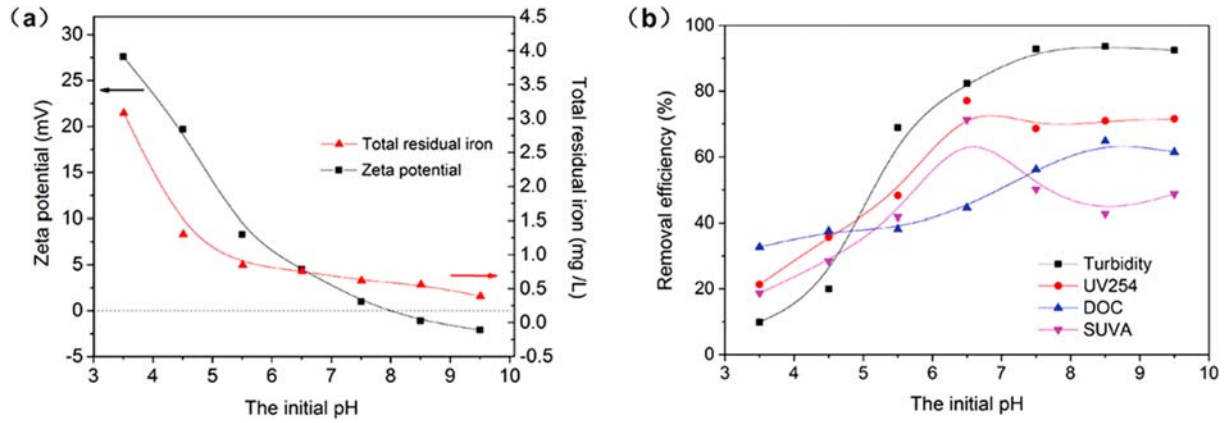

Fig. 11. Effect of initial pH value on the coagulation performance of surface water.

lized in water, resulting in large iron ion residuals. The coagulation performance for surface water as a function of the initial pH value is shown in Fig. 11(b). The removal of turbidity reaches the optimal value when the zeta potential of flocs approached isoelectric point, indicating that the turbidity removal is most efficient mainly by the mechanism of charge neutralization. The removal of UV_{254} and SUVA is found the most efficient at slight acidic pH value; in view of the content of Fe_b species at pH of 6.5 during coagulation mentioned in section 3.3.1, it can be concluded that charge neutralization and complexation ability of Fe_b was the most efficient for removing HHo which always suspends in surface water owing to the effect of electrostatic repulsion. Yet, the removal efficiency of DOC is the highest at the basic pH region where the Fe_c species are dominant. As a portion of DOC, the LHi is quite stable in water due to its hydration layer around the colloidal particles rather than the effect of the electrostatic repulsion [30]; it has been found the Fe_c species have the ability to destruct the liquid layer by strong adsorption [31], so the LHi is most likely removed by Fe_c species at the basic pH region.

CONCLUSION

(1) The SPFS with a high basicity and excellent solubility was synthesized by acid deficiency method. The total iron content of SPFS abtained was as high as 24.55% and the basicity was as high as 21.06% at R=0.2. An amorphous structure of the as-prepared SPFS was confirmed by XRD and SEM. The total content of Fe_b and Fe_c in the samples of $SPFS_{sto}$ was higher compared with that in the $LPFS_{sto}$ at the same value of R.

(2) Depolymerization and polymerization were verified to occur in the distribution of iron (III) species of $SPFS_{sto}$ during aging and dilution. The distribution of iron (III) species in the solution of $SPFS_{sto}$ with $[TFe] \geq 1.0 \times 10^3$ mg/L was stable and the average diameters of iron (III) species varied from 1.0 nm to 4.0 nm. Excessive hydrolysis occurred and massive Fe_c species or precipitates accumulated when 10 mg/L$<[TFe]<1.0\times10^3$ mg/L. When $[TFe] \leq 10$ mg/L, the Fe_c species would be degraded into the less polymerized species and the average diameters of iron (III) became more dispersed.

(3) The distribution of iron (III) species in the surface water depended on the dosage of PFS added and the initial pH value of surface water used in experiments. The content of Fe_b was much higher when the dosage of PFS was lower than 0.4 mM and the highly polymerized iron (III) species tended to dominate at the dosage range of 0.4-0.6 mM. Fe_a, Fe_b and Fe_c species dominated in acidic system, neutral system and basic system, respectively. Charge neutralization was the main mechanism for turbidity removal, while charge neutralization and complexation by Fe_b species was the most efficient for removal of HHo, and the absorption and sweeping capabilities of Fe_c cannot be neglected in removing LHi.

In summary, all of the results above enable a bright prospect for the applications of the high basicity SPFS synthesized by acid deficiency method as an effective coagulant in water supply field thanks to its innocuity and outstanding efficiency. Additionally, the high basicity SPFS is also expected to be used in the wastewater field for its excellent treatment of organics.

ACKNOWLEDGEMENT

This article was funded by the National Key Research and Development Program of China (No. 2017YFC0210203-4) of China.

REFERENCES

1. W. P. Cheng, *Colloid Surf., A*, **182**, 57 (2001).
2. D. Jia, M. Li, G. Liu, P. Wu, J. Yang, Y. Li, S. Zhong and W. Xu, *Colloids Surf., A: Physicochem. Eng. Asp.*, **512**, 111 (2017).
3. Y. Zhang, S. Guo, J. Zhou, C. Lin and G. Wang, *Chem. Eng. Process.: Process Intensification*, **49**, 859 (2010).
4. M. H. Fan, S. W. Sung, R. C. Brown, T. D. Wheelock and F. C. Laabs, *J. Environ. Eng-Asce*, **128**, 483 (2002).
5. A. I. Zouboulis, P. A. Moussas and F. Vasilakou, *J. Hazard. Mater.*, **155**, 459 (2008).
6. X. Zhang, X. Wang, Q. Chen, Y. Lv, X. Han, Y. Wei and T. Xu, *ACS Sustain. Chem. Eng.*, **5**, 2292 (2017).
7. J. Li, X. Liu, S. Wang, Z. Du, Y. Guo and F. Cheng, *J. Chem. Technol. Biotechnol.*, **93**, 365 (2018).
8. Y. Wei, J. Lu, X. Dong, J. Hao and C. Yao, *Korean J. Chem. Eng.*, **34**, 2641 (2017).
9. W. Chen, H. Zheng, H. Teng, Y. Wang, Y. Zhang, C. Zhao and Y.

Liao, *Plos One*, **10**, e0137116 (2015).
10. Y. Sun, X. Xiong, G. Zhou, C. Li and X. Guan, *Sep. Purif. Technol.*, **115**, 198 (2013).
11. H. Dong, B. Gao, Q. Yue, S. Sun, Y. Wang and Q. Li, *Chem. Eng. J.*, **258**, 442 (2014).
12. G. Lei, J. Ma, X. Guan, A. Song and Y. Cui, *Desalination*, **247**, 518 (2009).
13. H. Dong, B. Gao, Q. Yue, H. Rong, S. Sun and S. Zhao, *Desalination*, **335**, 102 (2014).
14. H. Rong, B. Gao, R. Li, Y. Wang, Q. Yue and Q. Li, *Chem. Eng. J.*, **243**, 169 (2014).
15. W. Xu and B. Gao, *J. Membr. Sci.*, **415**, 153 (2012).
16. Q. Yue, J. Miao and B. Gao, *Res. Environ. Sci.*, **15**, 17 (2002).
17. S. Bhattacharjee, *J. Control Release,* **235**, 337 (2016).
18. J. Q. Jiang and N. J. D. Graham, *J. Chem. Technol. Biot*, **73**, 351 (1998).
19. Y. J. Zheng, Z. Q. Gong, L. H. Liu and B. Z. Chen, *Transactions of Nonferrous Metals Society of China*, **12**, 983 (2002).
20. B. Gao, B. Liu, T. Chen and Q. Yue, *J. Hazard. Mater.*, **187**, 413 (2011).
21. H.-Z. Zhao, C. Liu, Y. Xu and J.-R. Ni, *Chem. Eng. J.*, **155**, 528 (2009).
22. Z. Bi, C. Feng, D. Wang, X. Ge and H. Tang, *Colloids Surf., A Physicochem. Eng. Asp.*, **416**, 73 (2013).
23. C. Yao and Y. Sun, *Environ. Chem.*, **10**, 1 (1991).
24. K. E. Lee, N. Morad, T. T. Teng and B. T. Poh, *Chem. Eng. J.*, **203**, 370 (2012).
25. Y. Wang, B. Gao, Q. Yue, J. Wei and Q. Li, *Chem. Eng. J.,* **142**, 175 (2008).
26. H. Hellman, R. S. Laitinen, L. Kaila, J. Jalonen, V. Hietapelto, J. Jokela, A. Sarpola and J. Ramo, *J. Mass Spectrom.: JMS*, **41**, 1421 (2006).
27. W. P. Cheng, *Sep. Sci. Technol.*, **36**, 2265 (2001).
28. B. Wang, Y. Shui, M. He and P. Liu, *Biochem. Eng. J.*, **121**, 107 (2017).
29. M. Yan, D. Wang, J. Ni, J. Qu, C. W. K. Chow and H. Liu, *Water Res.*, **42**, 3361 (2008).
30. M. Yan, D. Wang, J. Qu, J. Ni and C. W. Chow, *Water Res.,* **42**, 2278 (2008).
31. A. Fratiello, V. Kubo, S. Peak, B. Sanchez and R. E. Schuster, *Inorg. Chem.,* **10**, 393 (2002).